

## Autofluorescence imaging system to discriminate and quantify the distribution of benthic cyanobacteria and diatoms

Cátia Carreira,<sup>\*1,2</sup> Marc Staal,<sup>2</sup> Mathias Middelboe,<sup>2</sup> Corina P.D. Brussaard<sup>1,3</sup>

<sup>1</sup>Department of Biological Oceanography, NIOZ - Royal Netherlands Institute for Sea Research, PO Box 50, 790 AB Den Burg, Texel, The Netherlands

<sup>2</sup>Section for Marine Biology, University of Copenhagen, Strandpromenaden 5, 3000 Helsingør, 6 Denmark

<sup>3</sup>Aquatic Microbiology, Institute for Biodiversity and Ecosystem Dynamics, University of Amsterdam, Amsterdam, The Netherlands

### Abstract

Observation of benthic photoautotrophs on sediment surfaces shows a single algal layer without distinction between photosynthetic groups. Until now it has not been possible to distinguish between benthic photosynthetic microorganisms, i.e. cyanobacteria and diatoms, at  $\mu\text{m}$  to  $\text{mm}$  scales using a single nondisruptive system. Chlorophyll autofluorescence can be used to distinguish different photoautotrophic groups if the correct excitation light is applied. Using this principle, a nonintrusive technique was developed to study the spatial distribution of benthic cyanobacteria and diatoms. By means of a charge coupled device camera, diatoms and cyanobacteria could be identified by blue light (470 nm) excitation and amber light (600 nm) excitation, respectively. By this approach, diatom or cyanobacterial dominance could be easily distinguished using the blue over amber ratio. We applied this method successfully to (mixed) laboratory cultures as well as natural photosynthetic microbial mats. Cultures of the diatom *Nitzschia capitellata* and the cyanobacterium *Geitlerinema* sp. showed close correlation between autofluorescence and cell abundance. This simple and cheap imaging system allows fast observations of the fine-scale ( $\mu\text{m}$ – $\text{mm}$ ) spatial heterogeneities of live benthic microbial photoautotrophs both in culture and natural photosynthetic biofilms structure (e.g., microphytobenthos and photosynthetic microbial mats). © 2014 Association for the Sciences of Limnology and Oceanography

Photosynthetic microbial mats are productive ecosystems (Canfield et al. 2005), with a photosynthetic layer composed of a mixture of cyanobacteria and diatoms (Jørgensen et al. 1983; Mir et al. 1991). Using imaging pulse amplitude modulation, it is possible to detect the presence and distribution of photoautotrophs, but the technique does not distinguish between different photoautotrophic groups. Although high performance liquid chromatography (Brotas et al. 2003) and microscopy allow the identification of photoautotrophic groups, both techniques are relatively time consuming. Combining these analysis techniques with core slicing at high resolutions, e.g., 100  $\mu\text{m}$ , can give an indication of the vertical structure of the photoautotrophic groups. However, this approach is not very practical and prone to errors (due to small sample size). Moreover, because of the need for subsamples, it takes away the possibility for temporal analysis. There is thus need for an alternative fast and nondisruptive method. This method should discriminate between major

benthic photosynthetic groups, while showing spatial distribution and temporal development.

Cyanobacteria and diatoms are the most common photoautotrophic microorganisms in benthic systems (Brotas and Plante-Cuny 1998; Mir et al. 1991) with different compositions of accessory pigments (Campbell et al. 1998; Jeffrey et al. 2005). Although autofluorescence always occurs via chlorophyll *a* (Chl *a*), different wavelengths can be used to excite the accessory pigments, thus allowing discrimination of different algal groups based on the excitation light applied. Cyanobacteria absorb light in the yellow, orange, and red area of the visible spectrum using a combination of phycobiliproteins (Campbell et al. 1998). The most common phycobiliproteins are phycocyanin and phycoerythrin. Phycoerythrin occurs in cyanobacteria as well as in red algae and has a wide absorption peak ranging from 500 to 575 nm, while phycocyanin are exclusively found in cyanobacteria absorbing in the orange range (590–640 nm; Van Den Hoek et al. 1995). Diatoms absorb blue and red light with Chl *a*, Chl *c*, and fucoxanthin ( $\sim 450\text{nm}$ ; Van Den Hoek et al. 1995; Jeffrey et al. 2005). Green microalgae can also use blue

\*Correspondence: ccd.carreira@gmail.com

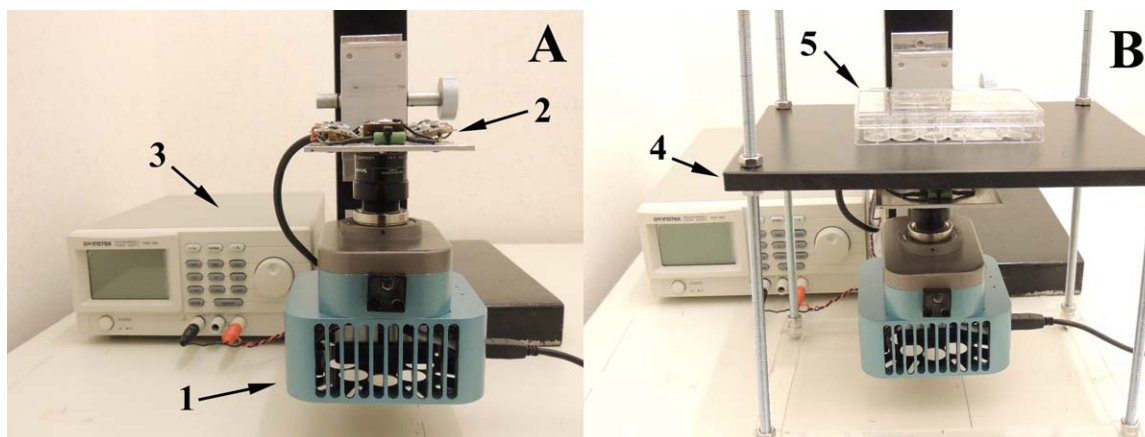


**Fig. 1.** Autofluorescence imaging system with CCD cooled camera setup (A) showing the (1) CCD camera (2) LEDs and (3) LED power supply. The imaging system (B) shows the (4) support structure for photoautotrophs culture measurements and (5) the microwell plate with photoautotrophs culture samples.

light and thus compete with diatoms. However, although green microalgae have been found in benthic systems (Baranguet et al. 1997), diatoms are generally more common in intertidal photosynthetic microbial mats (Mir et al. 1991).

Here we present a fast, simple, and nonintrusive method based on the difference in fluorescence excitation of the different photoautotrophic groups that allows determining microscale variability in spatial distribution and quantification of the two major primary producers of photosynthetic microbial mats, i.e., cyanobacteria and diatoms.

### Material and procedures

An imaging system was built using a cooled charge coupled device (CCD) 16 bits camera (1360 × 1024 pixels; TCC-1.4LICE Monochrome, Tucsen Imaging Technology Co. Ltd, China), cooled to  $-30^{\circ}\text{C}$  (below ambient temperature) with a ring of three blue (peak emission at 470nm; LXHL-MB1D, Lumileds, The Netherlands) and three amber (peak emission at 597 nm; LXHL-ML1D, Lumileds, The Netherlands) 1 W LEDs positioned around the lens (Fig. 1). The near infrared filter in front of the code chip was removed by unscrewing the glass in front of the code chip. Blue and amber lights were chosen as these excite fucoxanthin and phycocyanin pigments, characteristic of diatoms and cyanobacteria, respectively. A long-pass infrared filter (695 nm, IF092, Schneider-Kreuznach, Germany) was placed on top of the lens (Xenoplan 1.4/17cm, 17 mm focal length, C-mount, Schneider-Kreuznach, Germany) allowing Chl *a* autofluorescence ( $\sim 685$  nm) to be captured. The camera was connected to a computer, and the software TSVIEW 7.1.1.5 (Tucsen Imaging Technology Co. Ltd., China) was used to capture the images. The camera was connected to a manual one-dimensional (1D) manual vertical stage allowing the camera to be accurately moved up and down. The method was

initially tested on cultures of the diatom *Nitzschia capitellata* and the cyanobacterium *Geitlerinema* sp. Single and mixed populations were exposed to blue and amber light excitation. A rack was built to support the plate with organisms under observation. It consisted of a “table type” of setup (4 legs and a top) with a hole in the middle allowing the passage of light and to capture the images (Fig. 1B). It also allowed up and down adjustment. The focal distance of the lens was between 5 and 20 cm. With a focal distance of 5 cm, the observation area was  $4.5 \times 3.4$  cm ( $L \times W$ ) resulting in a resolution of  $30 \mu\text{m}$  per pixel, and if 20 cm was the focal distance, the monitored area was  $7 \times 5.3$  cm with a resolution of  $51 \mu\text{m}$  per pixel. Exposure times were chosen so that there were no over-saturated pixels or photobleaching and were typically around 400 ms. Samples were adapted to the dark for 5 min before excitation light was applied. Two autofluorescence photos were taken per sample. One photo with blue excitation light and one photo with amber excitation light to distinguish between diatoms and cyanobacteria, respectively. The relative dominance of the different photoautotrophic groups was obtained by dividing the blue autofluorescence image over the amber autofluorescence image (blue amber ratio; BAR). Thereafter, the ratio image was log transformed to make the scale linear. The calculated BAR indicates cyanobacterial dominance when negative, and diatom dominance when positive. Image analysis and calculations were performed using the freeware imaging software Image J 1.47m (<http://imagej.nih.gov/ij/>).

To test the relation between abundance and autofluorescence intensity of photoautotrophs, growth curves were made with cultures of the diatom *N. capitellata* and the cyanobacteria *Geitlerinema* sp. The photoautotrophs were kept in  $f/2$  media, at  $100 \mu\text{mol quanta m}^{-2} \text{s}^{-1}$  in a 16 : 8 h L : D cycle at  $20^{\circ}\text{C}$ . *N. capitellata* and *Geitlerinema* sp. were grown separately in 24-microwell plates (Greiner Bio-one) for 9–15

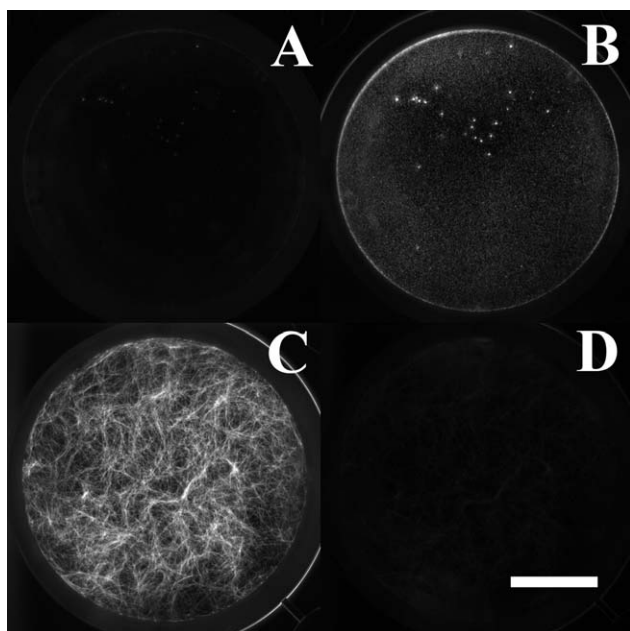


**Fig. 2.** Autofluorescence images of single populations of the diatom *N. capitellata* (A, B) and cyanobacterium *Geitlerinema* sp. (C, D) in culture. Autofluorescence after amber light excitation (A, C), and after blue light excitation (B, D). Scale bar is 1 cm.

days (until stationary phase). Blue and amber autofluorescence photos of 8 wells (each containing 1 mL) were taken daily at ambient temperature in a dark room. Every day, images were taken of the same four wells, and to four extra wells (in a total of 8 wells per day) that were daily destructively sampled, fixed with Lugol, and kept in the dark, until counts within 1–3 weeks. Counts were performed in a Sedgewick-Rafter chamber using a light microscope (Zeiss Axiophot) at  $\times 200$ – $400$  magnification. At least 400 cells were counted per sample. To determine the autofluorescence in the wells, we excluded all pixels that were not fluorescent by setting a threshold. We then selected a circle of 660 pixels in the center of the well and measured the number of fluorescent pixels and their intensity.

Application of the method to natural samples was tested using photosynthetic microbial mat samples from the Wadden Sea Island Schiermonnikoog, The Netherlands. With a knife, squares of  $15 \times 8 \times 4$  cm ( $L \times W \times H$ ) were cut out from the sediment and placed inside plastic boxes and taken to the laboratory within 3–4 h. Samples were kept under in situ conditions until use within 1–2 days. The photosynthetic microbial mats were exposed to blue and amber excitation light and the images analyzed as described above.

Linear regression analyses were performed to obtain the best-fitting coefficients between counts and autofluorescence, and prior to statistical analysis, normality was checked and the confidence level was set at 95% (Sokal and Rohlf 1995). The statistical analysis was conducted in SigmaPlot 12.0.

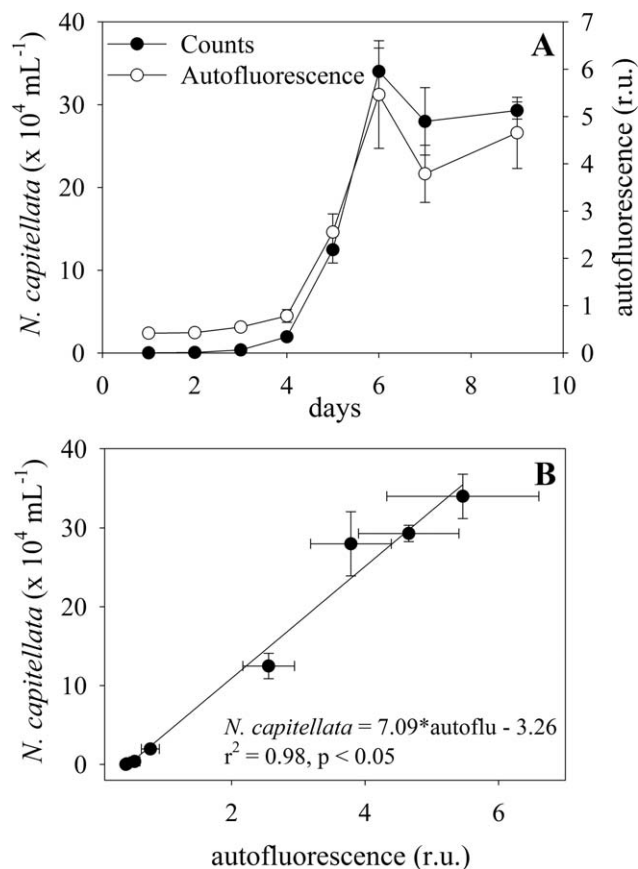


**Fig. 3.** Autofluorescence and cell counts of the diatom *N. capitellata*. (A) Temporal dynamics of average abundance (filled circles) and autofluorescence after blue light excitation (open circles), and (B) linear regression of *N. capitellata* autofluorescence with counts ( $r^2 = 0.98$ ,  $p < 0.05$ ). The standard deviations are shown ( $n = 4$ ).

### Assessment

Imaging of single populations of *N. capitellata* and *Geitlerinema* sp. after exposure to amber and blue light (Fig. 2) showed that *N. capitellata* autofluorescence is only observed with blue light excitation (Fig. 2A,B), and *Geitlerinema* sp. is only observed with amber light excitation (Fig. 2C,D). Therefore, blue light does not excite the cyanobacterium *Geitlerinema* sp., and amber light does not excite the diatom *N. capitellata*, allowing to clearly distinguishing between the two photoautotrophic groups.

Simultaneous autofluorescence measurements and cell counts of *N. capitellata* during growth in culture experiments showed comparable temporal dynamics in the two parameters (Fig. 3A), and, consequently, a strong linear correlation ( $r^2 = 0.98$ ,  $p < 0.05$ , Fig. 3B). *Geitlerinema* sp. autofluorescence and cell counts showed a similar development until day 8, after which the autofluorescence decreased and the cell abundance eventually reached a plateau (Fig. 4A). *Geitlerinema* sp. abundance showed a significant linear correlation with autofluorescence during the first 8 days ( $r^2 = 0.99$ ,

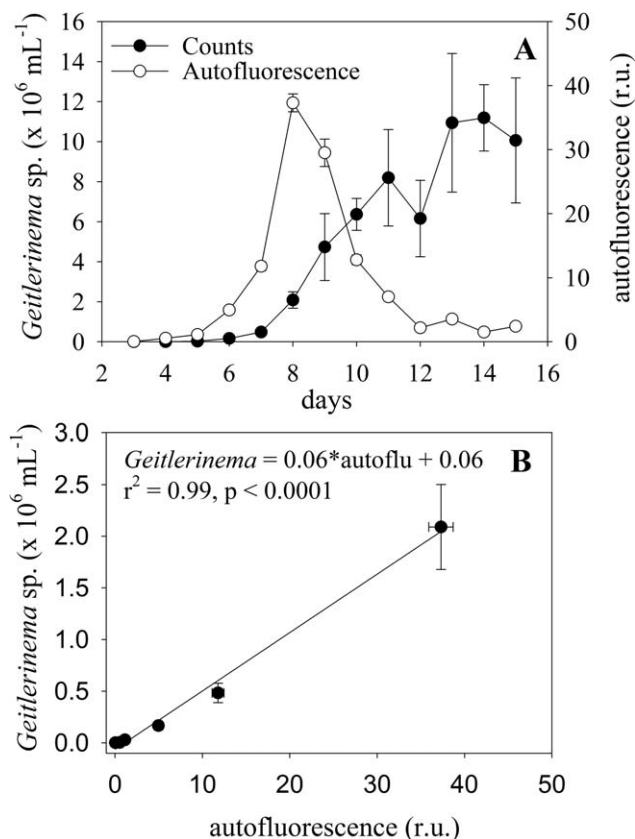


**Fig. 4.** Autofluorescence and cell counts of the cyanobacterium *Geitlerinema* sp. (A) temporal dynamics of average abundance (filled circles) and autofluorescence after amber light excitation (open circles), and (B) linear regression of *Geitlerinema* sp. autofluorescence with counts ( $r^2 = 0.99$ ,  $p < 0.0001$ ) of the first 8 days. The standard deviations are shown ( $n = 4$ ).

$p < 0.0001$ , Fig. 4B). However, after day 8, the relationship between counted cells and autofluorescence was lost, since the autofluorescence decreased while cell numbers in the wells still increased. In several of the wells *Geitlerinema* sp. filaments got detached from the bottom and floated at the surface out of the camera's focus plane. When fluorescing cells moved out of focal plane it resulted in lower fluorescence intensity. The number of wells in which filaments started to float increased with time. Moreover, an increasing amount of filaments were observed growing on the side walls of the wells after day 9. Both floating filaments and wall growth could not be captured by the 2D camera (Fig. 5) as the setup of the camera was developed for benthic systems.

Standard color photo observations of the mixed cultures (Fig. 6A) did not allow discrimination between *Geitlerinema* sp. and *N. capitellata*. When using blue excitation light, the diatom *N. capitellata* fluoresced showing a spatial distribution in the edge of the well it grew in (Fig. 6B). The cyanobacterium *Geitlerinema* sp. fluoresced when using amber light and showed a more patchy distribution (Fig. 6C). The BAR image displayed the distinct distribution pattern of both

diatom and cyanobacterium (Fig. 6D). BAR values  $< 0$  indicate dominance of *Geitlerinema* sp., while values  $> 0$  indicate diatom dominance. BAR values ranged from  $-1.83$  to  $1.98$ , with an average of  $0.16 \pm 0.45$ . Although there was on average no overall dominance of either species, on microscale, distinct dominance of either species could be clearly detected (Fig. 6E).

Observation of the color image of a photosynthetic microbial mat showed a greenish surface without obvious spatial patterns in photoautotrophs distribution (Fig. 7A). However, after blue (Fig. 7B) and amber (Fig. 7C) light excitation, strong microscale heterogeneity in spatial distribution of diatoms and cyanobacteria could be discriminated. BAR imaging showed a detailed distribution pattern of dominance of either photosynthetic group (Fig. 7D). The BAR along a cross section of the microbial mat (Fig. 7D) showed a distinct patchy distribution of these two key benthic photoautotrophs. The small-scale spatial heterogeneity in the dominance of either cyanobacteria or diatoms was observed at pixel level (Fig. 7E).

## Discussion

Using the blue and amber lights as excitation colors in combination with a monochromatic camera, we were able to discriminate between cyanobacteria and diatoms in mixed cultures and natural populations even with a relative low resolution of the camera CCD chip. A CCD camera, rather than a photodiode, was used to investigate the spatial component of the distribution of the different photoautotrophic groups. Several imaging systems (i.e., Waltz, PSI) for imaging of photosynthetic performances of plants, photosynthetic biofilms, and unicellular algae are commercially available (Oxborough et al. 2000; Ralph et al. 2005; Aldea et al. 2007). However, the macroimagers of these types have only one excitation color and cannot be used for spatial differentiation of photosynthetic groups in mats, and only measure the photosynthetic performance of one of the photoautotrophic groups. In heterogeneous systems like photosynthetic microbial mats, differences in photosynthetic performance of selected areas can be caused by physiological factors or by a variation in dominance of different photoautotrophic groups. To discriminate between these two factors, it is necessary to separate the individual algal groups which require the use of different excitation colors within a single imaging system. Beutler et al. (2002) have used a submersible probe with different excitation colors to distinguish between phytoplankton groups, but without visual images. Other imaging systems (Polerecky et al. 2009; Trampe et al. 2011) have been built that can be mounted on a microscope, which can excite benthic microbial photoautotrophs at different colors. However, although such microscopy systems allow both visualizing and quantifying the autofluorescence in mixed population systems, the field of view in our system is much

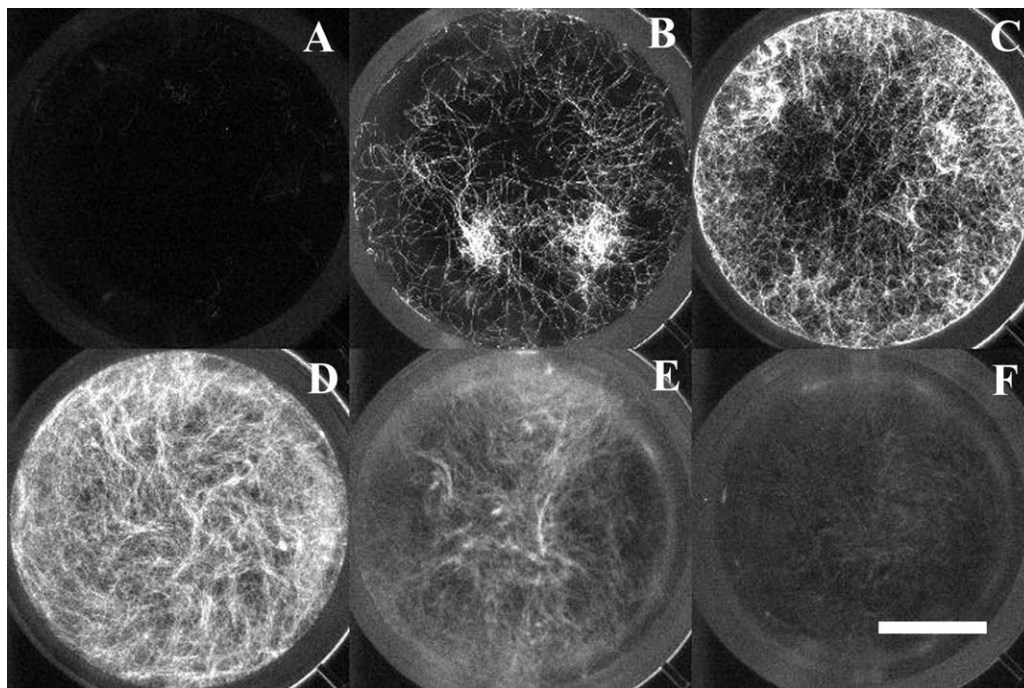


**Fig. 5.** Autofluorescence images of *Geitlerinema* sp. growth at days 3, 5, 7, 9, 11, and 13 (A–F). After a week, the cells detached from the bottom which negatively affected the quality of the autofluorescence images as the floating cells were out of the plane of focus of the camera. Scale bar is 1 cm.

wider (15–37 cm<sup>2</sup>) than what can be obtained in a microscope (0.01–0.96 mm<sup>2</sup>), while still acquiring fine resolution ( $\mu\text{m}$ ) information. Furthermore, the transport of a microscope with an attached camera is less practical and more costly than our system, which only needs a camera and light source (~\$2500; Table 1). The objective of this system is to determine population distribution of different benthic microbial photoautotrophs which is not possible under the microscope, and without destroying the samples (both in field and in laboratory experiments). Finally, as our imaging system uses few optical elements it has high transmission of light, increasing sensitivity and may allow visualization of single filaments that may not be visible using a standard compound microscope. The system described in this study can be easily converted to suit field studies just by mounting the set up in a dark box with an opening of the field of view on the sediment site and the addition of a portable power supply. Quantification of the two ecologically important photoautotrophs was tested by comparing their specific autofluorescence with their biomass in the form of cell abundance. Culture experiments showed that autofluorescence was a good indicator of abundance for both the diatom *N. capitellata* and the cyanobacterium *Geitlerinema* sp., as long as cells stayed attached to the bottom of the wells (in the plane of focus). This shows that the camera system is a good indicator of cell abundance in systems where all biomass is present in the focal plane. We used a lens with a short focal distance (5 cm, with a macro ring) that resulted in a relatively

thin focal plane. With our settings, the 16-bit gray value increased by 1600 for the *Geitlerinema* sp. filaments, corresponding to the 4- $\mu\text{m}$  thickness of the filaments. The highest gray values were around 62,000 (found at day 8), indicating that layers of up to 35 filaments thick can be measured with this method, equivalent to at least 140  $\mu\text{m}$  depth. It is expected that excitation levels decrease with depth in the biofilm layer due to absorbance of the excitation light. Using a linear extrapolation, the thickness of the layer will likely be underestimated. Usually the photosynthetically active microbial mat layer is on the order of a few hundred  $\mu\text{m}$ , however, in sandy sediments there may be substantial light at deeper layers (order of mm; Kühl and Jørgensen 1992; Al-Najjar et al. 2012).

Although we did not observe significant amounts of green microalgae in the studied microbial mats, the possible interference from green microalgae when obtaining the diatom autofluorescence may be solved using an additional green color to excite Chl *b* present in green microalgae but not in diatoms (Van Den Hoek et al. 1995). Thus, using a ratio of blue over green autofluorescence, it is possible to distinguish between diatoms and green microalgae distribution.

This study used the well-known phenomenon by which specific excitation colors of algal pigments can distinguish different photosynthetic groups in a new imaging approach to quantify the spatial distribution of cyanobacteria and diatoms in photosynthetic mats. Furthermore, the use of the BAR allows the rapid identification of areas of dominance of

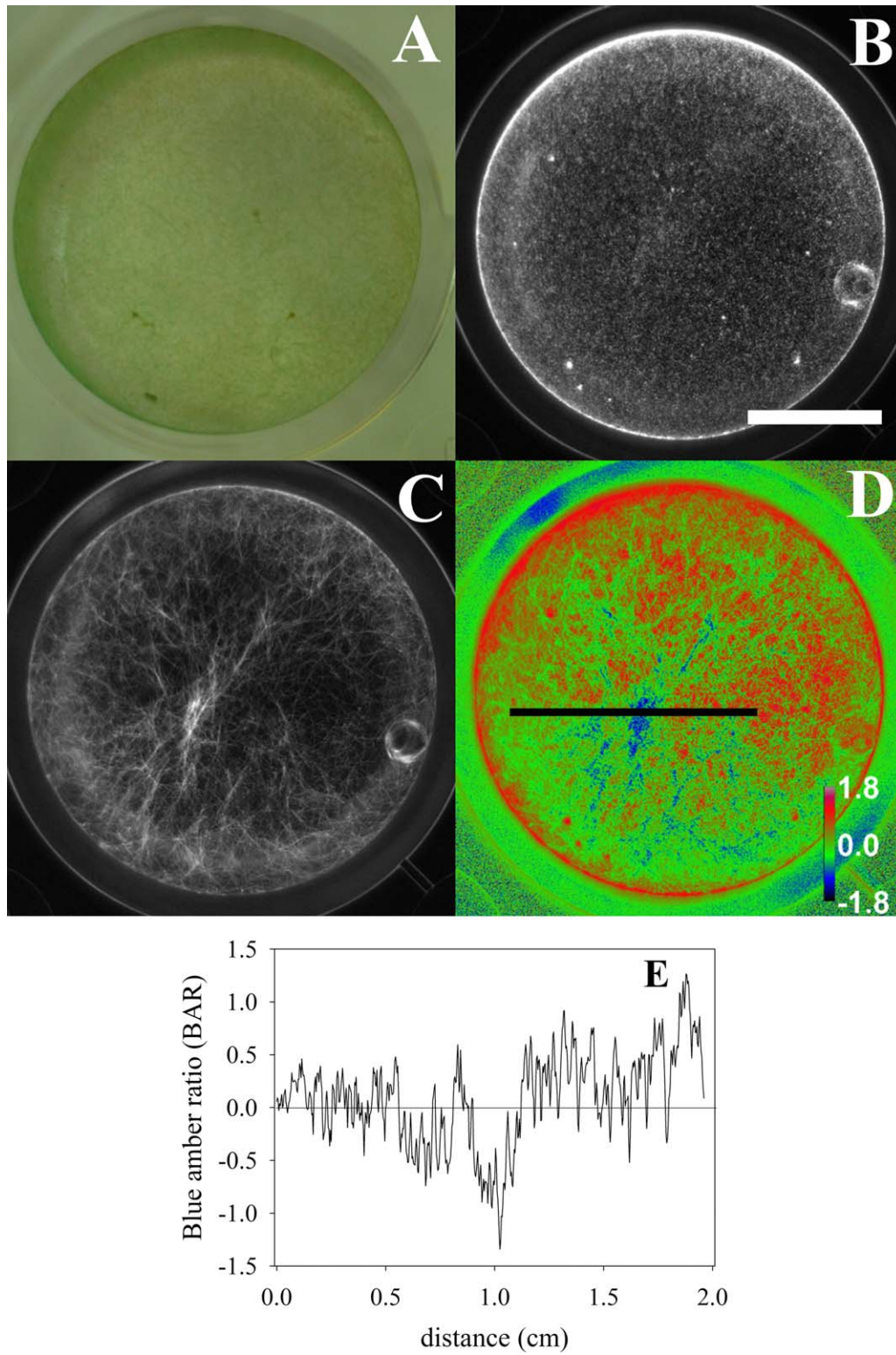


**Fig. 6.** Mixed populations of the diatom *N. capitellata* and cyanobacterium *Geitlerinema* sp. in culture: (A) Standard color camera image; (B) autofluorescence after blue light exposure, (C) autofluorescence after amber light exposure; (D) Blue amber ratio (BAR), and (E) BAR values along a cross section indicated by the 2-cm black line in figure D. Scale bar is 1 cm.

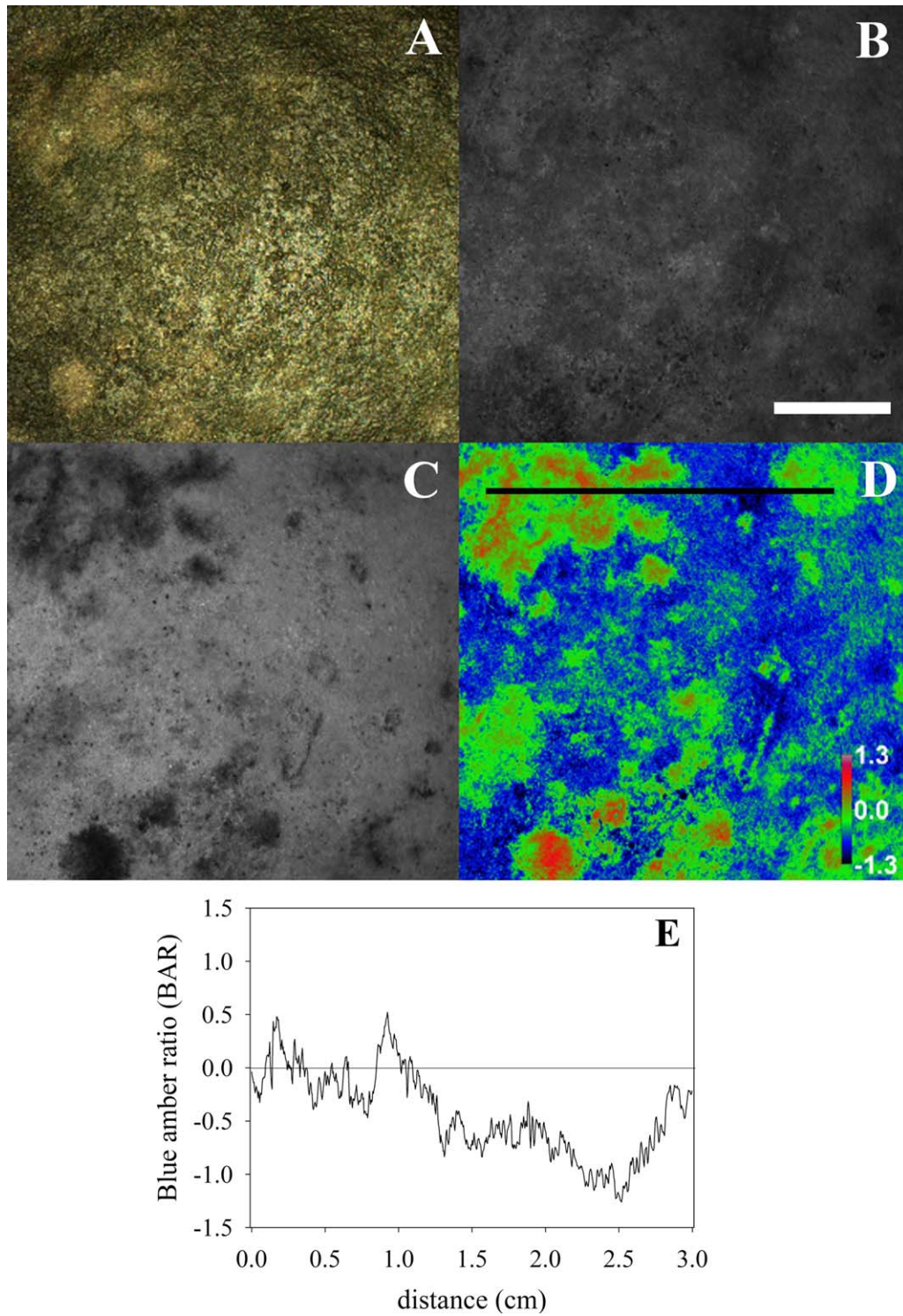


**Fig. 7.** Photosynthetic microbial mat from the tidal Wadden Sea island Schiermonnikoog, The Netherlands by (A) Standard color image; (B) autofluorescence after blue light exposure, (C) autofluorescence after amber light exposure; (D) Blue amber ratio (BAR), and (E) BAR values along a cross section indicated by the 3-cm black line in figure D. Scale bar is 1 cm.

**Table 1.** Brand, series, and price (USD) information of the material used to setup the autofluorescence imaging system

Material	Brand/series	Price (USD)
CCD camera	Tucsen Imaging Technology Co. LTD, TCC-1.4LICE mono cooled	1085
Lens	Schneider-Kreuznach, Xenoplan 1.4/17 cm	850
Long pass filter	Schneider-Kreuznach, IF 092, 695 nm	92
LED	Luxeon 1watt, ×3 blue (470 nm) and ×3 Amber (597)	2.5–5 each
Power supply	GW Instek programmable power supply PSP-405	400
<i>Software</i>		
TSView	7.1.1.5	Provided with the camera
ImageJ	1.47 m	Freeware

either cyanobacteria or diatoms in mixed laboratory culture and in natural photosynthetic microbial mats.

Composition, distribution, and quantification of the biomass of specific photoautotrophic groups are important parameters in most ecological and ecophysiological studies. Until now, the horizontal spatial distribution of the different groups of photoautotrophs in microbial mats have been inferred from vertical profiles (Jørgensen et al. 1983; Mir et al. 1991) and the maximum spatial resolution was limited to the centimeter scale at best. Using different light excitations and collecting the autofluorescence, we could resolve the spatial heterogeneity and quantify the distribution of living diatoms and cyanobacteria in culture and in field samples at the  $\mu\text{m}$ –mm scale. Since this technique is nonintrusive, it has a high potential for studies on population dynamics on spatial and temporal scales which are relevant for microbial communities. Furthermore, it is easy to build a mobile system that can be applied to field studies for in situ measurements.

## References

- Al-Najjar, M. a. A., D. D. Beer, M. Kühl, and L. Polerecky. 2012. Light utilization efficiency in photosynthetic microbial mats. *Environ. Microbiol.* **14**: 982–992, doi:10.1111/j.1462-2920.2011.02676.x
- Aldea, M., T. D. Frank, and E. H. Delucia. 2007. A method for quantitative analysis of spatially variable physiological processes across leaf surfaces. *Photosynth. Res.* **90**: 161–172, doi:10.1007/s11120-006-9119-z
- Barranguet, C., P. M. J. Herman, and J. J. Sinke. 1997. Microphytobenthos biomass and community composition studied by pigment biomarkers: Importance and fate in the carbon cycle of a tidal flat. *J. Sea Res.* **38**: 59–70, doi:10.1016/S1385-1101(97)00032-4
- Beutler, M., K. H. Wiltshire, B. Meyer, C. Moldaenke, C. Lüring, M. Meyerhöfer, U.-P. Hansen, H. Dau. 2002. A fluorometric method for the differentiation of algal populations in vivo and *in situ*. *Photosynth. Res.* **72**: 39–53, doi:10.1023/A:1016026607048
- Brotas, V., and M. R. Plante-Cuny. 1998. Spatial and temporal patterns of microphytobenthic taxa of estuarine tidal flats in the Tagus Estuary (Portugal) using pigment analysis by HPLC. *Mar. Ecol. Prog. Ser.* **171**: 43–57, doi:10.3354/meps171043
- Brotas, V., N. Risgaard-Petersen, J. Serôdio, L. Ottossen, T. Dalsgaard, and L. Ribeiro. 2003. In situ measurement of photosynthetic activity and respiration of intertidal benthic microalgal communities undergoing vertical migration. *Ophelia* **57**: 13–26, doi:10.1080/00785236.2003.10409502
- Campbell, D., V. Hurry, A. K. Clarke, P. Gustafsson, and A. G. Oquist. 1998. Chlorophyll fluorescence analysis of cyanobacterial photosynthesis and acclimation. *Microbiol. Mol. Biol. Rev.* **62**: 667–683.
- Canfield, D. E., B. Thamdrup, and E. Kristensen. 2005. *Aquatic Geomicrobiology*. Elsevier, doi:10.1016/S0065-2881(05)48017-7
- Jeffrey, S. W., R. F. C. Mantoura, and T. Bjørnland. 2005. Data for the identification of 47 key phytoplankton pigments, p. 449–596. *In* S. W. Jeffrey, R. F. C. Mantoura and S. W. Wright [eds.], *Phytoplankton pigments in oceanography: Guidelines to modern methods*. UNESCO Publishing.
- Jørgensen, B. B., N. P. Revsbech, and Y. Cohen. 1983. Photosynthesis and structure of benthic microbial mats: Microelectrode and SEM studies of four cyanobacterial communities. *Limnol. Oceanogr.* **28**: 1075–1093, doi:10.4319/lo.1983.28.6.1075
- Kühl, M., and B. B. Jørgensen. 1992. Spectral light measurements in microbenthic phototrophic communities with fiber-optic microprobe coupled to a sensitive diode array detector. *Limnol. Oceanogr.* **37**: 1813–1823, doi:10.4319/lo.1992.37.8.1813
- Mir, J., M. Martinez-Alonso, I. Esteve, and R. Guerrero. 1991. Vertical stratification and microbial assemblage of a microbial mat in the Ebro Delta (Spain). *FEMS Microbiol. Ecol.* **86**: 59–68, doi:10.1111/j.1574-6968.1991.tb04795.x
- Oxborough, K., A. R. M. Hanlon, G. J. C. Underwood, and N. R. Baker. 2000. In vivo estimation of the photosystem II photochemical efficiency of individual microphytobenthic cells using high-resolution imaging of chlorophyll *a* fluorescence. *Limnol. Oceanogr.* **45**: 1420–1425, doi:10.4319/lo.2000.45.6.1420
- Polerecky, L., A. Bissett, M. Al-Najjar, P. Faerber, H. Osmers, P. A. Suci, P. Stoodley, D. de Beer. 2009. Modular spectral imaging system for discrimination of pigments in cells and microbial communities. *Appl. Environ. Microbiol.* **75**: 758–771, doi:10.1128/AEM.00819-08

- Ralph, P. J., U. Schreiber, R. Gademann, M. Kühl, and A. W. D. Larkum. 2005. Coral Photobiology Studied with a New Imaging Pulse Amplitude Modulated Fluorometer1. *J. Phycol.* **41**: 335–342, doi:[10.1111/j.1529-8817.2005.04034.x](https://doi.org/10.1111/j.1529-8817.2005.04034.x)
- Sokal, R. R., and F. J. Rohlf [eds.]. 1995. *Biometry the principles and practice of statistics in biological research*, 3rd Edition ed. W. H. Freeman and Company.
- Trampe, E., J. Kolbowski, U. Schreiber, and M. Kühl. 2011. Rapid assessment of different oxygenic phototrophs and single-cell photosynthesis with multicolour variable chlorophyll fluorescence imaging. *Mar. Biol.* **158**: 1667–1675, doi:[10.1007/s00227-011-1663-1](https://doi.org/10.1007/s00227-011-1663-1)
- Van Den Hoek, C., D. G. Mann, and H. M. Jahns. 1995. *Algae, An introduction to phycology*. Cambridge University Press.

### **Acknowledgements**

We thank the NIOZ Marine Technology group for technical assistance and Tim Piel for help during the development of the autofluorescence imaging system. We also thank two anonymous reviewers for their constructive comments on the manuscript. The study received financial support from Fundação para a Ciência e a Tecnologia (FCT) – SFRH/BD/43308/2008, from the Royal Netherlands Institute for Sea Research (NIOZ), and the Danish Council for Independent Research.

*Submitted 31 March 2014*

*Revised 10 January 2015*

*Accepted 20 January 2015*

*Associate editor: Prof. Gordon Taylor*